9th International Conference on

Steel and Aluminium Structures (ICSAS19)

Bradford, UK, 3-5, July, 2019

# OPTIMUM DESIGN OF COLD-FORMED STEEL BEAMS SUBJECT TO BENDING, SHEAR AND WEB CRIPPLING

**R. DOBSON[a], K. POOLOGANATHAN[a], S. GUNALAN[b], P. GATHEESHGAR[a], J. YE[c] and L. MA[a]**

[a] Faculty of Engineering and Environment, University of Northumbria, Newcastle, UK

Emails: ross.dobson@northumbria.ac.uk, Keerthan.pologanathan@northumbria.ac.uk, g.perampalam@northumbria.ac.uk, ma.luo@northumbria.ac.uk

[b] School of Engineering and Built Environment, Griffith University, Brisbane, Australia

Email: s.gunalan@griffith.edu.au

[b] Department of Architecture and Civil Engineering, University of Bath, Bath, Australia

Email: J.Ye@bath.ac.uk

**Keywords**: Cold-formed Steel Beams; Finite Element Analysis; Optimum Design; Bending; Shear and Web Crippling

***Abstract***. *Recently, cold-formed steel (CFS) members have become more prevalent within the construction industry. CFS beams can be optimised to increase their load carrying capacity. In this research, shape optimisation method is developed to obtain high structural resistance of cold-formed steel beams by taking into account the bending, shear and web crippling actions. First, the flexural strengths of the sections are determined based on the effective width method adopted in EC3, while the optimisation process is performed using the Particle Swarm Optimisation (PSO). Five different CFS channel cross-section are considered in the optimisation process. The flexural strengths of the optimised sections are then verified using detailed nonlinear finite element analysis. The results indicated that the optimised CFS beams provide a bending capacity which is up to 50% higher than the conventional CFS channel sections with the same amount of material. Shear, web crippling behaviours of five optimised CFS beams were then investigated. Finally, innovative optimised CFS beam was proposed for lightweight forms of buildings and modular building systems to obtain high structural resistance.*

## 1 INTRODUCTION

The use of CFS members in low rise building construction and modular building systems has increased significantly in recent times. More than 70% of all steel building construction is expected to be cold-formed in the near future. In recent years, CFS cross-sections are increasingly being used as primary structural elements. For example, CFS framing systems are used in low- to mid-rise multi-storey buildings [1] and CFS portal frames are gaining popularity in single-storey industrial buildings [2,3]. Compared to hot-rolled members, CFS thin-walled members offer several advantages of economy and efficiency, including a high strength for a lightweight, a relatively straightforward manufacturing process and an ease of transportation and erection. Above all, CFS sections offer flexibility and versatility in producing a variety of cross-sectional shapes, which are obtained by bending relatively thin metal sheets using either

a cold-rolling or a press-braking process at room temperature. Figure 1 shows the commercially available CFS sections with complex shapes. The flexibility of the manufacturing process in obtaining various shapes means that there is a great potential for CFS sections to be optimized to meet specific objectives, thereby bringing practical benefits to both manufacturers and structural designers.

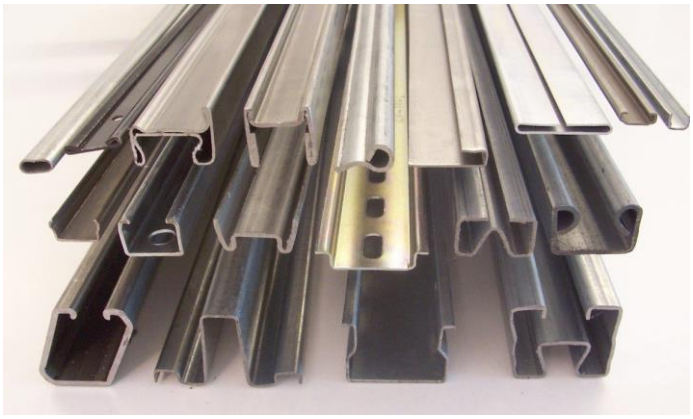

Figure 1: Commercially available CFS sections with complex shapes

Due to their typically large flat width-to-thickness ratios, CFS sections are inherently susceptible to local, distortion and global buckling modes, resulting in a complex optimisation process. Previous studies on the optimisation of CFS elements have mainly been limited to varying the dimensions of standard cross-sections such as lipped channel beams [4], channel columns with and without lips [5,6] and hat, I- and Z- cross-section CFS beams [7]. Taking the elastic buckling strength as an optimisation criterion, [8,9] developed optimum CFS beams with a monosymmetrical open cross-section and sinusoidally corrugated flanges, as well as optimum I-shaped sections with box-shaped flanges.

More recently, CFS compression and bending members [10, 11] were optimised with respect to their capacity according to EC3 (CEN, 2005) [12] using Genetic Algorithms. The researchers investigated the influence of the column length and the shift of the effective centroid, induced by local/distortional buckling, on the optimal design solutions. The shapes of the cross-section were thereby limited to the conventionally used lipped channels.

In order to obtain ‘global optimum’ solutions, research at Johns Hopkins University and Griffith University was conducted on the free-form optimisation of CFS cross-sections without placing any prior constraints on the shape of the cross-section. The finite strip method (FSM) and the direct strength method (DSM) were thereby combined with Genetic Algorithms (GA) to obtain optimum shapes for open CFS cross-section columns [13, 14, 15]. While this led to some innovative new geometries, the resulting cross sections were not ‘pre-qualified’ according to the DSM approach, thus casting some doubt on the optimisation procedure. Additionally, these studies did not consider any manufacturing or construction constraints and, therefore, highly complex shapes were obtained which cannot be deemed suitable for practical applications due to a complex manufacturing process and the obvious difficulty in connecting the cross-section to other elements. This work by incorporating some end-user constraints and by limiting the numbers of rolling passes in the manufacturing process. CFS columns with different lengths were optimised and more practical shapes were obtained, which, however, still did not meet the DSM prequalification criteria [16].

This study aims to develop optimum cold-formed steel beams in bending, shear and web crippling. In total, five different CFS channel cross-section are considered in the optimisation

process. All sections are optimised by maximising the cross-sectional flexural, shear and web crippling capacity for a given thickness and coil width (equal to the total developed length of the cross-section).

UK's construction sector has been followed by rising costs, low productivity and a heavy reliance on traditional building methods. UK lags behind countries in Europe, North America and Asia with a modular building sector in its infancy. It has been reported that the UK government are planning a new wave of modular building in a drive to solve Britain's housing crisis. More than 100,000 modular homes could be constructed as the UK government looks at ways to meet its target to provide a million new homes by 2020. Hence there is a need to develop a lightweight modular building with enhanced structural performance. Figures 2 and 3 show the application of cold-formed steel sections in modular building systems. Optimum cold-formed steel beams considered in this research study can be used in lightweight forms of building constructions and modular building system.

Figure 2: Light steel framework of a module

Figure 3: High-rise modular building, Manchester, UK

## 2 PARTICLE SWARM OPTIMISATION (PSO)

Particle swarm optimisation (PSO) is a population-based method which is inspired by the swarming behaviour of biological populations such as the motion of bird flocks or schools of fish [17]. Its mechanism has some parallels with evolutionary computation techniques, such as Genetic Algorithms (GA). An initial population of solutions is randomly generated, but unlike GA, solutions are optimised by updating generations without any evolution operators such as crossover or mutation. The potential solutions in PSO, called particles, move in the problem space by following the current optimum particles. This usually leads to a better efficiency in terms of computational time and cost and, therefore, a faster convergence rate compared to GA [18,19].

A swarm comprises N particles moving around a D-dimensional search space, in which each particle represents a potential solution to the optimisation problem. The position and velocity vectors of ith particle are $\rho = \{\rho_{i1}, \rho_{i2}, ..., \rho_{ij}, ..., \rho_{iD}\}$ and $Vi = \{v_{i1}, v_{i2}, ... , v_{ij}, ... , v_{iD}\}$, respectively, where i = 1, 2, 3, ... N. The particles fly through the feasible region in search for the global optimal solution. In each iteration step, the ith particle updates its position and velocity based on a combination of (a) its personal best position over its history, and (b) the position of the particle within the swarm with the best position in the previous iteration.

The optimisation procedure in this research study aimed to maximise the bending capacity (Section Moment Capacity) of cold-formed steel cross-sections. The optimisation problem can be expressed as:

$$\max(M_{c,Rd} = W_{eff}(x).f_y) \qquad d_{\min} \le x_i \le d_{\max} \tag{1}$$

where $M_{c,Rd}$ is the moment resistance of a cross-section about its major axis and $W_{eff}$ (x) is the effective section modulus. The effective section modulus $W_{eff}$ is calculated about the major principal axis through the centroid of the effective area. The effective width and the effective thickness of each plate element are first calculated according to the procedure outlined in Eurocode 3, Part 1.3 to account for both local and distortional buckling. The effective second moment of area of the cross section $I_{eff}$ is then calculated from the contributions of all effective parts of the cross-section and divided by the maximum distance from the effective centroid to the edge of the cross-section to obtain $W_{eff}$. For each design variable, $x_i$, lower and upper bounds, $d_{min}$ and $d_{max}$, were determined based on a combination of the constraints imposed by EC3 (CEN, 2005) [12] and certain manufacturing limitations and practical considerations, which will be explained further in this section. Throughout the optimisation process, the thickness of the cross sections was kept constant at 1.5 mm and the total developed length of the cross-section (the coil width) was also maintained at 415 mm. These values were taken from a commercially available channel section, shown in Figure 4, which was used as a benchmark and to which the performance of the optimised sections will be compared in this section.The values of the radius of the rounded corners (measured along the heart-line), the elastic modulus and the Poisson's ratio were taken as 3 mm, 210 GPa and 0.3, respectively. The yield stress of the CFS material was assumed to be $f_y$ = 450 MPa. It is again noted that the optimisation was carried out with respect to the cross-sectional capacity, excluding lateral-torsional buckling. This situation is representative, for instance, of purlins connected to a steel deck with concrete topping, where the compression flange is continuously supported, or even of roof purlins where the lateral and rotational stiffness of the roof diaphragm and/or the presence of sufficient bridging prevent any out-of-plane effects.

EC3 (CEN, 2005) [12] design rules also impose certain limits on the plate width-to-thickness ratios, the relative dimensions of the cross-section and the angle of the edge stiffeners. These constraints were also taken into account in the optimisation procedure. One of the major advantages of the PSO algorithm is that these constraints can easily be accommodated and others added. The constraints merely result in a restriction of the search space of the particle swarm.

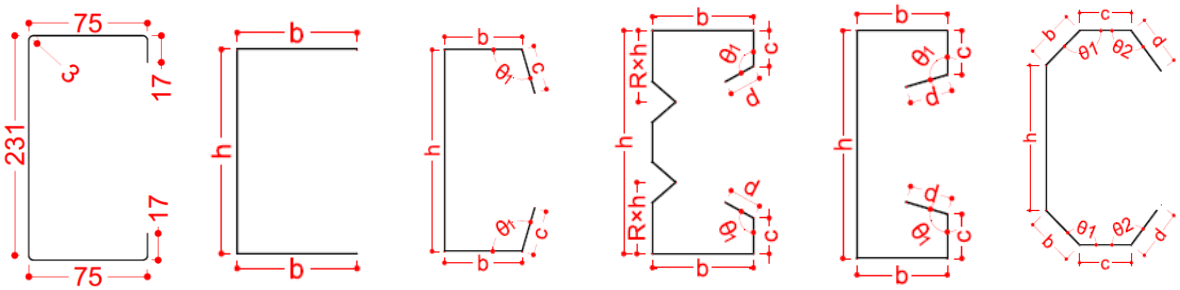


Figure 4: Benchmark section and selected prototypes (dimensions in mm)

To facilitate the optimization process, both the design procedure and the optimization algorithm were implemented in Matlab [20]. The population size of the particle swarm N was taken as 100, and 100 iterations $k_{max}$ were used to obtain the optimum results. The maximum and minimum inertial weight factors $w_{max}$ and $w_{min}$ were taken as 0.95 and 0.4, respectively. Each of the prototypes was optimized 3 times using a different set of random initial particles

and the results with the maximum bending capacity were retained as the optimum section. Table 1 shows the geometrical details and section moment capacities of the optimized CFS beams.

Table 1: Geometrical details and section moment capacities (Bending) of the optimized CFS beams

| Prototypes | h | b | c | d | $\theta_1$ | $\theta_2$ | R | Ms (kNm) |
|---|---|---|---|---|---|---|---|---|
| LCB (Standard) | 231 | 75 | 17 | - | - | - | - | 10.30 |
| 1 (UCB) | 315 | 50 | - | - | - | - | - | 9.84 |
| 2 (LCB) | 270 | 50 | 23 | - | 90 | - | - | 13.38 |
| 3 | 232 | 50 | 25 | 6.5 | 135 | - | 0.1 | 13.41 |
| 4 | 242 | 50 | 29 | 7.5 | 90 | 95 | - | 15.11 |
| 5 | 185 | 48 | 50 | 17 | 105 | - | - | 16.12 |

## 3 FINITE ELEMENT MODELS

Detailed geometric and material non-linear finite element analyses were performed using ABAQUS Version 6.14 to evaluate the flexural behaviour and capacity of the optimised cross-sections for the five considered prototypes (see Table 1) as well as the standard lipped channel beams. The main purposes of the finite element analyses were: (a) to examine the accuracy of the method proposed in Section 2 for the flexural design of folded-flange cross sections; and (b) to investigate the overall effectiveness of the developed optimisation framework in obtaining sections with increased bending capacity (section moment capacity).

Additional nonlinear finite element analyses were also performed using ABAQUS to investigate the shear and web crippling behaviour and capacity of the optimised cross-sections for the five considered prototypes. The centreline dimensions were used to model the optimised cold-formed steel beams in ABAQUS using middle surface shell offset definition.

### 3.1 Bending

The FE models were developed in ABAQUS using the general-purpose S4R element (Figure 6). This element is a 4-node quadrilateral shell element with reduced integration. Through a sensitivity analysis, a mesh size of 5 mm x 5 mm for the flat plate sections, with smaller elements used in the rounded corner sections was found to be appropriate.

The effects of geometric imperfections were included in the FE analysis by scaling the local and distortional modes to specific amplitudes and superposing them onto the initial perfect geometry. The boundary conditions and the applied loading are shown in Figure 6 while Figure 7 shows the FE model of the folded-flange beam (Prototype 5) subjected to bending.

To simulate pin-ended boundary conditions with prevented warping (consistent with the assumptions made in the optimisation process), the nodes of each end section of the CFS member were coupled to the central point of the web (acting as the master node). The external load was then applied in the form of uniform rotations of the end sections about the major axis, using a displacement control regime. Large deformation effects were included in the element formulation and a geometric nonlinear analysis was carried out in order to be able to accurately track the post-buckling behaviour of the CFS beams. It is worth mentioning that the modelling techniques utilised in this study, including the type of elements, the material behaviour, the meshing and the imperfection modelling borrow heavily from the work by [21,22]. These techniques have been extensively verified against experimental results (Schafer, 2003 and 2006), demonstrating excellent predictive capability with an average error typically less than

4%. Table 2 shows the comparison of the section moment capacities (bending) of the optimised and standard sections obtained from EC3 and FE analysis.

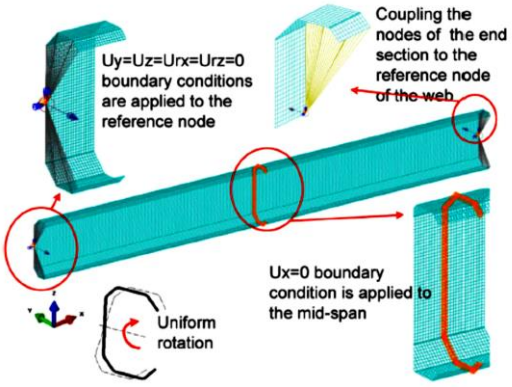


Figure 6: FE model of the folded-flange beam (prototype 5) subjected to bending

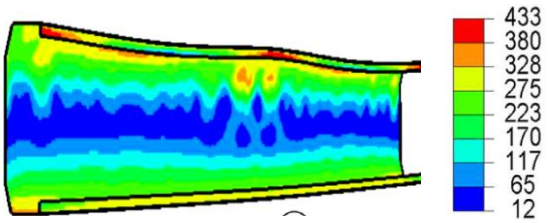


Figure 7: Bending failure mode of optimized CFS beam (prototype 5)

Table 2: Comparison of the section moment capacities (bending) of the optimized and standard sections obtained from EC3 and FE analysis

| Prototypes | $M_s$(kNm) (EC3) | $M_s$(kNm) (FEM) | FEM/EC3 |
|---|---|---|---|
| LCB (Standard) | 10.30 | 10.4 | 0.99 |
| 1 (UCB) | 9.84 | 9.11 | 1.08 |
| 2 (LCB) | 13.38 | 12.73 | 1.05 |
| 3 | 13.41 | 12.33 | 1.09 |
| 4 | 15.11 | 14.09 | 1.07 |
| 5 | 16.12 | 15.52 | 1.04 |
| Mean | | | 1.05 |
| COV | | | 0.034 |

### 3.2 Shear

This section describes the development of finite element (FE) models to investigate the shear behaviour of optimised cold-formed steel beams. For this purpose, a general-purpose finite element program, ABAQUS, was used. Appropriate parameters were chosen for the geometry, mechanical properties, loading and support conditions. FE models of simply supported single optimised cold-formed steel beams with shear centre loading. ABAQUS has several element types to simulate the shear behaviour of optimised cold-formed steel beams. In this study, shell element was selected as it has the capability to simulate the elastic buckling and nonlinear ultimate shear behaviour of thin steel beams. The shell element S4R in ABAQUS was used to model the optimised cold-formed steel beams.

Two methods of analysis were used. Bifurcation buckling analyses were first used to obtain the eigenvectors for the inclusion of initial geometric imperfections in non-linear static analysis. Non-linear static analyses including the effects of large deformation and material yielding were then employed to investigate the shear behaviour and strength of optimised cold-formed steel beams until failure. In this study, the required numbers of elements to model flange and web elements of optimized cold-formed steel beams were chosen based on convergence studies. These convergence studies showed that in general, the use of element sizes of approximately 5 mm x 5 mm was able to simulate the shear buckling and yielding deformations and provided accurate shear capacity results for all the sections. The geometry and finite element mesh of optimised cold-formed steel beams are shown in Figure 8.

A perfect plasticity model was adopted in all the FE models with nominal yield stresses. Previous studies showed that the use of measured strain hardening in the web element in finite element analyses (FEA) improved the shear capacity by less than 1% [23]. Hence strain hardening was not included in the analyses. The elastic The elastic modulus and Poisson's ratio were taken as 200 GPa and 0.3, respectively. Simply supported boundary conditions were implemented as given below in the FE models of optimised cold-formed steel beams. Here, $u_x$, $u_y$ and $u_z$ are translations and $\theta_x$, $\theta_y$ and $\theta_z$ are rotations in the x, y and z directions, respectively.

| | | |
|---|---|---|
| Left and right supports: | $u_x$ = restrained | $\theta_x$ = free |
| | $u_y$ = restrained | $\theta_y$ = free |
| | $u_z$ = free | $\theta_z$ = restrained |
| Mid-span loading point: | $u_x$ = restrained | $\theta_x$ = free |
| | $u_y$ = free | $\theta_y$ = free |
| | $u_z$ = restrained | $\theta_z$ = restrained |
| Strap Location*:* | $u_x$ = restrained | $\theta_x$ = free |
| | $u_y$ = free | $\theta_y$ = free |
| | $u_z$ = free | $\theta_z$ = restrained |

Figure 8 shows the applied loads and boundary conditions of the FE model while Figure 9 depicts the shear failure mode of optimised cold-formed steel beam (Prototype 3). The point load and simply supported boundary conditions were used at the shear centre using a fixed node to eliminate twisting of the section (see Figure 10). The vertical translation was not restrained at the loading point. Full height web side plates were modelled as 20 mm thick rigid plates.

The magnitude of local imperfections was taken as $0.006d_1$ for all optimised cold-formed steel beams [24]. The critical imperfection shape was introduced using the *IMPERFECTION option in ABAQUS. Preliminary FEA showed that the effect of residual stresses on the shear capacity of cold-formed steel beams is less than 1%. Hence the residual stresses were not considered in the FEA of optimised cold-formed steel beams.

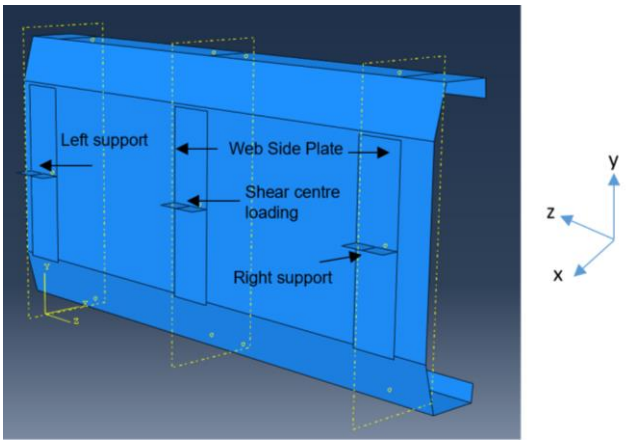


Figure 8: FE model of the folded-flange beam (Prototype 5) subjected to shear failure

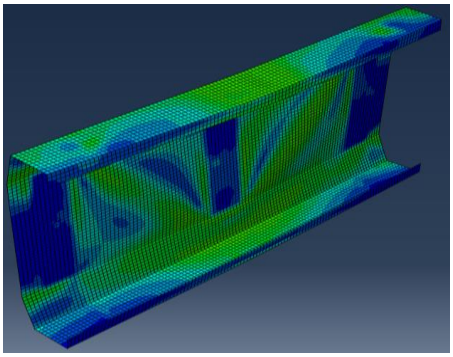

Figure 9: Shear failure mode of optimized CFS beam (Prototype 5)

### 3.3 Web crippling

In this section, the finite element models were developed to simulate the web crippling behaviour of optimized cold-formed steel beams under ITF load cases. Finite element models were developed using ABAQUS and analysed using the quasi-static analysis method. The quasi-static analysis was used to overcome the possible convergence and contact difficulties faced in the non-linear static analysis of the web crippling behaviour of optimized cold-formed steel beams. Three-dimensional deformable S4R shell elements were used to model optimized cold-formed steel beams while loading and support bearing plates and web side plates were all modelled using four node rigid body elements R3D4. The web and flange elements of optimized cold-formed steel beams were modelled using 5 mm x 5 mm elements except at the corners. The optimized cold-formed steel beams' inside bent radius has a significant influence on its web crippling behaviour thus more elements are needed to model the corners. Hence 1 mm x 5 mm elements were used to model the corners as shown in Figure 10. Rigid body elements used to model web side plates and loading and support bearing plates were 10 mm x 10 mm as their sizes do not influence the web crippling behaviour. The ABAQUS classical metal plasticity model was used in all the analyses. Since analyses are based on quasi-static method, the modelled elements need to have mass or inertia values. Therefore, the typical steel density of 7850 kg/m3 (7.85x10-9 tonne/mm$^3$ in ABAQUS) was used here.

Boundary conditions were assigned to the reference points of loading and support bearing plates. Figures 10 show the boundary conditions applied to optimized cold-formed steel beams subject to ITF load case. The loading plate at the top was assigned displacement control using smooth step amplitude to impose smooth loading on the flange of the optimized cold-formed

steel beam. The loading plate was free to move vertically while its vertical displacement was limited to 20 mm. Translations along both lateral and longitudinal axes and rotation about the longitudinal axis of the loading plate were restrained. Simply supported condition was simulated at the bottom support plates by using pin and roller boundary conditions in the support bearing plates. ie. as shown in Figure 10, translations of support plate-1 in all three directions and rotation about the longitudinal (z) axis were restrained to simulate pin support while translation of support plate-2 along lateral (x) and longitudinal (z) axis and rotation about longitudinal (z) axis were restrained. Lateral axis translation was restrained at quarter points.

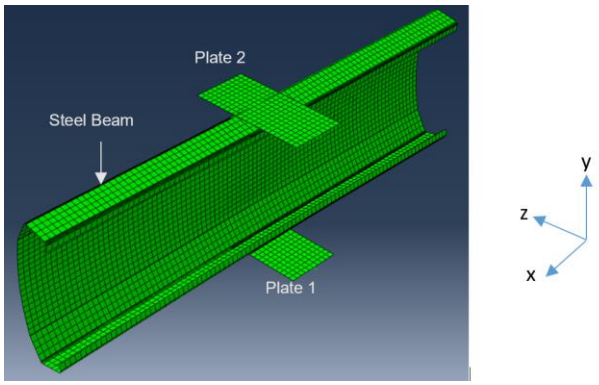


Figure 10: FE model of the folded-flange beam (Prototype 5) subjected to web crippling (ITF load)

In the models used here, surface-to-surface contact was assigned between the shell FE model representing optimized cold-formed steel beams and the rigid plates representing bearing plates. Separations were allowed between the contact surfaces after the initial contact. The friction between contact surfaces was set to 0.4 and contact surfaces were assigned to hard surfaces using hard contact pressure overclosure. The quasi-static analytical option was chosen in this study. Past and recent studies also used a quasi-static analysis method in their web crippling studies as improved analytical approach [25,26,27,28,29]. Displacement rate of 0.7 mm/minute was considered until failure. Figure 11 depicts the web crippling failure mode of the optimised folded-flange beam.

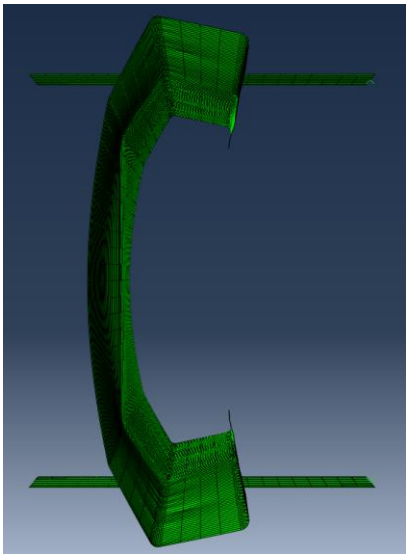

Figure 11: Web crippling failure mode (ITF load case) of optimized CFS beam (Prototype 5)

## 4 RESULTS

Table 3 shows the bending, shear and web crippling capacities of optimised and standard cold-formed steel beams from FEA. It elaborates the increased efficiency of the proposed folded-flange prototype (Prototype 5) compared to any other prototype considered. It is shown that, for the same amount of material, prototype 5 leads to a maximum flexural capacity which is around 50% higher than the standard commercially available channel section. Folded-flange sections are also easy to manufacture and connect to typical floor systems and modular building system and, hence, are suitable for practical CFS beam sections. However, it was found that shear and web crippling capacities of the proposed folded-flange prototype (Prototype 5) reduced by 15% and 55%, respectively when it compared with standard commercially available channel section.

Table 3 shows that for the same amount of material, Prototype 4 leads to a higher flexural capacity which is around 35% higher than the standard commercially available channel section. Prototype 4 sections are also easy to manufacture and connect to typical floor systems and modular building system and, hence, are suitable for practical CFS beam sections. It was found that the shear and web crippling capacities of proposed Prototype 4 did not reduce when it compared with standard commercially available channel section.

Table 3: Finite element analyses results

| Prototypes | Bending(Section Moment Capacity) (kNm) $M_s$ | $M_s$ (%) | Shear Capacity (kN) $V_v$ | $V_v$ (%) | Web Crippling Capacity (kN) $R_b$ | $R_b$ (%) |
|---|---|---|---|---|---|---|
| LCB (Standard) | 10.4 | 100% | 53.7 | 100% | 14.06 | 100% |
| 1 (UCB) | 9.11 | 88% | 42.86 | 80% | 12.59 | 90% |
| 2 (LCB) | 12.73 | 122% | 54.32 | 101% | 14.67 | 104% |
| 3 | 12.33 | 119% | 53.86 | 100% | 14.69 | 104% |
| 4 | 14.09 | 135% | 53.45 | 100% | 14.63 | 104% |
| 5 | 15.52 | 149% | 45.93 | 86% | 6.35 | 45% |

## 5 CONCLUSIONS

This section describes the development of finite element (FE) models to investigate the shear behaviour of optimised cold-formed steel beams. For this purpose, a general-purpose finite element program, ABAQUS, was used. Appropriate parameters were chosen for the geometry, mechanical properties, loading and support conditions. FE models of simply supported single optimised cold-formed steel beams with shear centre loading. ABAQUS has several element types to simulate the shear behaviour of optimised cold-formed steel beams. In this study, shell element was selected as it has the capability to simulate the elastic buckling and nonlinear ultimate shear behaviour of thin steel beams. The shell element S4R in ABAQUS was used to model the optimised cold-formed steel beams.

It was found that the same amount of material, prototype 5 leads to a maximum flexural capacity which is around 50% higher than the standard commercially available channel section. Folded-flange sections are also easy to manufacture and connect to typical floor systems and modular building system and, hence, are suitable for practical CFS beam sections. However, it was found that shear and web crippling capacities of the proposed folded-flange prototype

(Prototype 5) reduced by 15% and 55%, respectively when it compared with standard commercially available channel section. It was found that section moment capacity of proposed prototype 4 increased by 35% and shear and web crippling capacities of proposed prototype 4 did not reduce when it compared with standard commercially available channel section. Optimised cold-formed steel beams (Prototypes 4 and 5) can be used in lightweight forms of building constructions and modular building system.

## REFERENCES


[1] Fiorino, L., Iuorio, O. and Landolfo, R., 'Designing CFS structures: The new school bfs in naples', *Thin-Walled Structures*, 78, 37-47, 2014.

[2] Lim, J. and Nethercot, D.A., 'Ultimate strength of bolted moment-connections between cold-formed steel members', *Thin-Walled Structures*, 41,1019-1039, 2003.

[3] Lim, J. and Nethercot, D.A., 'Finite element idealization of a cold-formed steel portal frame', *Journal of Structural Engineering*, 130,78-94, 2004.

[4] Lee, J., Kim, S., Park, H. and Woo, B. 'Optimum design of cold-formed steel channel beams using micro Genetic Algorithm', *Engineering Structures*, 27, 17-24, 2005.

[5] Tian, Y. and Lu, T., 'Minimum weight of cold-formed steel sections under compression', *Thin-Walled Structures*, 42, 515-532, 2004.

[6] Lee, J., Kim, S., and Seon Park, H., 'Optimum design of cold-formed steel columns by using micro-genetic algorithms', *Thin-Walled Structures*, 44, 952-960, 2006.

[7] Adeli, H. and Karim, A., 'Neural Network Model for Optimization of Cold-Formed Steel Beams', *Journal of Structural Engineering*, 123, 1535-1543, 1997.

[8] Magnucki, K., Maćkiewicz, M. and Lewiński, J., 'Optimal design of a mono-symmetrical open cross section of a cold-formed beam with cosinusoidally corrugated flanges', *Thin-Walled Structures*, 44, 554-562, 2006.

[9] Magnucki, K., Maćkiewicz, M. and Lewiński, J., 'Optimization of mono- and anti-symmetrical I-sections of cold-formed thin-walled beams', *Thin-Walled Structures*, 44, 832-836, 2006.

[10] Ma, W. Becque, J., Hajirasouliha, I. and Ye, J., 'Cross-sectional optimization of cold-formed steel channels to Eurocode 3', *Engineering Structures*, 101, 641-651, 2015.

[11] Ye, J., Hajirasouliha, I., Becque, J. and Eslami, A., 'Optimum design of cold-formed steel beams using Particle Swarm Optimisation method', *Journal of Constructional Steel Research*, 122, 80-93, 2016.

[12] CEN, Eurocode 3, 2005, Design of steel structures, part 1.3: general rules—supplementary rules for cold-formed steel members and sheeting, in, brussels: European committee for standardization.

[13] Leng, J. Z., Guest, J. K. and Schafer, B. W., 'Shape optimization of cold-formed steel columns', *Thin-Walled Structures*, 49, 1492-1503, 2011.

[14] Gilbert, B. P., Savoyat, T. J. M. and Teh, L. J., 'Self-shape optimisation application: Optimisation of cold-formed steel columns', *Thin-Walled Structures*, 60, 173-184, 2012.

[15] Liu, H., Igusa, T. and Schafer, B. W., 'Knowledge-based global optimization of cold-formed steel columns', *Thin-Walled Structures*, 42, 785-801, 2004.

[16] Leng, J. Z., Li, Z. J., Guest, J. K. and Schafer, B. W., 'Shape optimization of cold-formed steel columns with fabrication and geometric end-use constraints', *Thin-Walled Structures*, 85, 271-290, 2014.

[17] Carlos, C., Satchidananda, D. and Susmita, G. (Eds), S*warm Intelligence for Multi-objective Problems in Data Mining*, Springer, 2009.

[18] Hassan, R., Cohanim, B., De Weck, O. and Venter, G., 'A comparison of particle swarm optimization and the genetic algorithm', *Proceedings of the 1st AIAA Multidisciplinary Design Optimization Specialist Conference*, 18 -21, 2005.

[19] Jeong, S., Hasegawa, S., Shimoyama, K. and Obayashi, S., 'Development and investigation of efficient GA/PSO-HYBRID algorithm applicable to real-world design optimization', *IEEE Computational Intelligence Magazine*, 4, 36-44, 2009.

[20] Mathworks, Matlab R 2011, in, Mathworks, Inc, 2011.

[21] Haidarali, M. R. and Nethercot, D. A., 'Finite element modelling of cold-formed steel beams under local buckling or combined local/distortional buckling', *Thin-Walled Structures*, 49, 1554-1562, 2011.

[22] Shifferaw, Y. and Schafer, B. W., 'Inelastic Bending Capacity of Cold-Formed Steel Members', *Journal of Structural Engineering*, 138, 468-480, 2012.

[23] Keerthan, P. and Mahendran, M., 'New design rules for the shear strength of LiteSteel beams', *Journal of Constructional Steel Research*, 67, 1050-1063, 2011.

[24] Keerthan, P. and Mahendran, M., 'Improved shear design rules for lipped channel beams with web openings', *Journal of Constructional Steel Research*, 97, 127-142, 2014.

[25] Kaitila, O., Web crippling of cold-formed thin-walled steel cassettes. PhD Thesis, Helsinki University of Technology, Finland, 2004.

[26] Natário, P., Silvestre, N. and Camotim, D., 'Web crippling failure using quasi-static FE models', *Thin-Walled Structures*, 84, 34-49, 2014.

[27] Natário, P., Silvestre, N. and Camotim, D., 'Computational modelling of flange crushing in cold-formed steel sections', *Thin-Walled Structures*, 84, 393-405, 2014.

[28] Sundararajah, L., Mahendran, M. and Keerthan, P., 'Experimental Studies of Lipped Channel Beams Subject to Web Crippling under Two-Flange Load Cases, *Journal of Structural Engineering*, 142, 2016.

[29] Sundararajah, L., Mahendran, M. and Keerthan, P., 'New design rules for lipped channel beams subject to web crippling under two-flange load cases', *Thin-Walled Structures*, 119, 421-437, 2017.